Indian Journal of Pure & Applied Physics
Vol. 53, March 2015, pp. 151-159

Vibrational spectroscopic investigation, first hyper polarizability and homo-lumo analysis of 2,2,4-tribromoacetophenone

S Jeyavijayan

Department of Physics, J J College of Engineering and Technology, Tiruchirappalli 620 009

E-mail: jaya_vijayan83@yahoo.com

Received 2 August 2014; revised 24 November 2014; accepted 23 January 2015

The FTIR and FT-Raman spectra of 2,2,4-tribromoacetophenone (TBAP) have been recorded in the regions 4000-400 cm^{-1} and 3500-50 cm^{-1}, respectively. Utilizing the observed FTIR and FT-Raman data, a complete vibrational assignment and analysis of the fundamental modes of the compound were carried out. The optimum molecular geometry, harmonic vibrational frequencies, infrared intensities and Raman scattering activities, were calculated by the density functional theory (DFT/B3LYP) method with 6-311++G(d,p) basis set. The difference between the observed and scaled wavenumber values of most of the fundamentals is very small. A detailed interpretation of the infrared and Raman spectra of TBAP is also reported based on potential energy distribution (PED). The calculated HOMO and LUMO energies show that charge transfer occurs within the molecule.

Keywords: FTIR, FT-Raman, DFT calculations, 2,2,4-tribromoacetophenone

1 Introduction

Acetophenone is one of the most typical aromatic carbonyl, which shows interesting photochemical properties[1,2]. Halogen combined acetophenone like 2,2,4-tribromoacetophenone (TBAP) possesses non-linear optics (NLO) properties[3]. NLO has wide applications in the field of telecommunication and optical information storage devices. The organic NLO materials play an important role in frequency mixing, electro-optic modulation, optical parametric oscillation and optical bi-stability. Because of these versatile behaviour of acetophenone, Anbarasu *et al*[4]., have extensively studied the scaled quantum study and vibrational spectra of 5-fluoro-2-hydroxyacetophenone. Seth *et al*[5]. investigated the spectroscopic and X-ray structure of ortho-hydroxy acetophenones. Pei *et al*[6]. investigated the Franck-Condon region photo-dissociation dynamics of *p*-nitroacetophenone using resonance Raman spectroscopy and density functional theory calculations. During the course of investigation on the samples of biological and pharmaceutical active compounds, the attention has been turned towards 2,2,4-tribromoacetophenone. The assignment of the vibrational frequencies for substituted acetophenone becomes a complicated problem because of the superposition of several vibrations due to fundamentals and substituents. However, a comparison of the spectra with that of the parent compound gives some definite clues about the nature of the molecular vibrations.

The vibrational spectra of the molecule 2,2,4-tribromoacetophenone have been studied completely and identified the various normal modes with greater wave numbers accurately. In the present study, the density functional theory (DFT) calculations have been performed to support the wave number assignments.

2 Experimental Details

The pure sample of TBAP obtained from Lancaster Chemical Company, UK and used as such for the spectral measurements. The room temperature Fourier transform infrared spectrum of the title compound is recorded in the region 4000-400 cm^{-1} at a resolution of ± 1 cm^{-1} using BRUKER IFS 66V model FTIR spectrometer equipped with an MCT detector, a KBr beam splitter and globar arc source.

The FT-Raman spectrum of TBAP is recorded on a computer interfaced BRUKER IFS 66V model interferometer equipped with FRA-106 FT-Raman accessories. The spectrum is measured in the Stokes region 3500-50 cm^{-1} using Nd: YAG laser operating at 200 mW power continuously with 1064 nm excitation. The reported wave numbers are expected to be accurate within ± 1 cm^{-1}.

3 Computational Details

In order to provide information with regard to the structural characteristics and the normal vibrational modes of TBAP, the DFT-B3LYP correlation functional calculations have been carried out. The entire calculations are performed using the GAUSSIAN 09W software package[7]. The DFT level calculations employing the Becke 3LYP keyword, which invokes Becke's three-parameter hybrid method[8] using the correlation function of Lee *et al.*[9], have been carried out with 6-311++G(d,p) basis set. All the parameters are allowed to relax and all the calculations converged to an optimized geometry which corresponds to true minimum, as revealed by the lack of imaginary values in the wavenumber calculations. The scaling of the force constants were performed according to SQM procedure[10,11] using selective scaling in the natural internal coordinate representation[12,13]. The vibrational problem was set-up in terms of internal and symmetry coordinates. To check whether the chosen set of symmetric coordinates contribute maximum to the potential energy associated with the molecule, the potential energy distribution (PED) has been carried out. The cartesian representation of the theoretical force constants has been computed at the fully optimized geometry by assuming C_1 point group symmetry. The symmetry of the molecule was also helpful in making vibrational assignment. The transformation of force field, the subsequent normal coordinate analysis including the least square refinement of the scale factors and calculation of the PED are done on a PC with the MOLVIB program (version V7.0-G77) written by Sundius[14,15]. By the use of GAUSSVIEW molecular visualization program[16] along with available related molecules, the vibrational frequency assignments were made by their PED with a high degree of confidence. The PED elements provide a measure of each internal coordinate's contributions to the normal coordinate.

4 Results and Discussion

4.1 Molecular geometry

The optimized molecular structure of TBAP is shown in Fig. 1. The optimization geometrical parameters of TBAP obtained by the DFT/B3LYP method with 6-311++G(d,p) basis set are listed in the Table 1. The title molecule has one C-O bond length, three C-Br bond lengths, five C-H bond lengths and eight C-C bond lengths. The carbon atom is bonded to

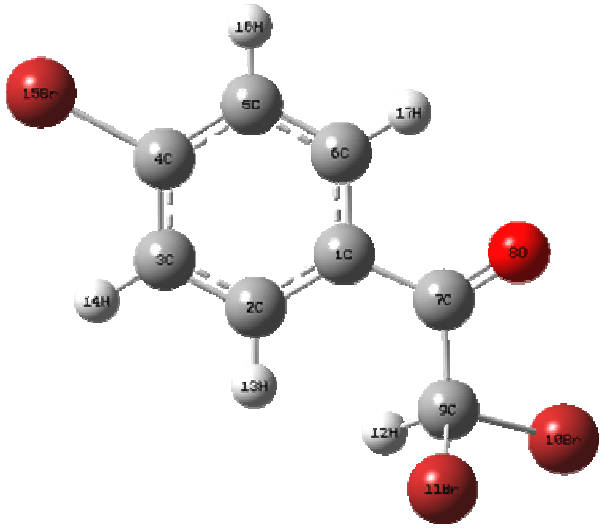

Fig. 1 — Molecular structure of 2,2,4-tribromoacetophenone

the hydrogen atom with σ-bond in TBAP and substitution of O=C–CBr_2H group instead of hydrogen atom reduces the electron density at the ring carbon atom. In the substituted benzene, the ring carbon atoms exert a large attraction on the valence electron cloud of the H atom resulting in an increase in the C–H force constant and a decrease in the corresponding bond length. In the present work, the C–H bond lengths were calculated as 1.082Å. According to the calculation, the order of the bond length is C5–C6 < C2–C3 < C3–C4 < C4–C5 < C1–C2 < C1–C6. From the order of the bond length, it is clear that the hexagonal structure of the benzene ring gets slightly distorted. This can be due to the influence of conjugation between the substituents and the ring. The C-C bond lengths adjacent to the O=C–CBr_2H group and C4-Br15 bonds increase and the angles C2-C1-C6 and C3-C4-C5 (118.79° and 121.21°, respectively by B3LYP/6-311++G(d,p) method) deviate from typical hexagonal angle of 120°. This is because of the effect of substitution of bromine atom attached to C4 of the ring and O=C–CBr_2H group attached to C1 of the ring. The calculated geometrical parameters are the basis for calculating other parameters such as vibrational frequencies and thermodynamics properties of the compound.

Detailed description of vibrational modes can be given by means of normal coordinate analysis. For this purpose, the full set of 59 standard internal coordinates (containing 14 redundancies) for the title

Table 1 — Optimized geometrical parametres of 2,2,4-tribromoacetophenone by DFT-B3LYP method with 6-311++G(d,p) basis set

Bond Length	Value (Å) B3LYP	Bond Angle	Value (°) B3LYP	Dihedrel Angle	Value (°) B3LYP
C1-C2	1.401	C2-C1-C6	118.79	C6-C1-C2-C3	0.09
C1-C6	1.403	C2-C1-C7	124.14	C6-C1-C2-H13	-178.44
C1-C7	1.496	C6-C1-C7	117.07	C7-C1-C2-C3	-179.42
C2-C3	1.391	C1-C2-C3	120.79	C7-C1-C2-H13	2.04
C2-H13	1.082	C1-C2-H13	121.23	C2-C1-C6-C5	-0.35
C3-C4	1.392	C3-C2-H13	117.96	C2-C1-C6-H17	179.82
C3-H14	1.082	C2-C3-C4	119.16	C7-C1-C6-C5	179.20
C4-C5	1.394	C2-C3-H14	120.41	C7-C1-C6-H17	-0.63
C4-Br15	1.910	C4-C3-H14	120.43	C2-C1-C7-O8	-175.94
C5-C6	1.387	C3-C4-C5	121.21	C2-C1-C7-C9	4.43
C5-H16	1.082	C3-C4-Br15	119.39	C6-C1-C7-O8	4.54
C6-H17	1.082	C5-C4-Br15	119.41	C6-C1-C7-C9	-175.09
C7-O8	1.207	C4-C5-C6	119.05	C1-C2-C3-C4	0.24
C7-C9	1.542	C4-C5-H16	120.39	C1-C2-C3-H14	-179.60
C9-Br10	1.944	C6-C5-H16	120.56	H13-C2-C3-C4	178.82
C9-Br11	1.977	C1-C6-C5	120.99	H13-C2-C3-H14	-1.02
C9-H12	1.082	C1-C6-H17	118.61	C1-C2-H13-Br11	32.79
		C5-C6-H17	120.40	C3-C2-H13-Br11	-145.79
		C1-C7-O8	121.82	C2-C3-C4-C5	-0.33
		C1-C7-C9	117.60	C2-C3-C4-Br15	179.75
		O8-C7-C9	120.58	H14-C3-C4-C5	179.51
		C7-C9-Br10	112.03	H14-C3-C4-B r15	-0.41
		C7-C9-Br11	107.72	C3-C4-C5-C6	0.08
		C7-C9-H12	113.21	C3-C4-C5-H16	-179.92
		Br10-C9-Br11	112.45	Br15-C4-C5-C6	-180.00
		Br10-C9-H12	105.97	Br15-C4-C5-H16	0.00
		C1-C9-H12	105.35	C4-C5-C6-C1	0.26
		C9-Br11-H13	56.71	C4-C5-C6-H17	-179.91
		C2-H13-Br11	111.03	H16-C5-C6-C1	-179.74
				H16-C5-C6-H17	0.10
				C1-C7-C9-Br10	150.33
				C1-C7-C9-Br11	-85.49
				D1-C7-C9-H12	30.57
				O8-C7-C9-Br10	-29.30
				O8-C7-C9-Br11	94.87
				O8-C7-C9-H12	-149.06
				C7-C9-Br11-H13	76.98
				Br10-C9-Br11-H13	-159.10
				H12-C9-Br11-H13	-44.13
				C9-Br11-H13-C2	-74.79

For numbering of atom refer Fig. 1

compound are defined in Table 2. From these, a non-redundant set of local symmetry coordinates is constructed by suitable linear combinations of internal coordinates following the recommendations of Fogarasi *et al*[12,13]. are summarized in Table 3.

4.2 Vibrational assignments

From the structural point of view the molecule is assumed to have C_1 point group symmetry and hence, all the calculated frequency transforming to the same symmetry species (A). The molecule consists of 17 atoms and expected to have 45 normal modes of vibrations. The detailed vibrational assignments of fundamental modes of TBAP along with the PED %, calculated IR intensities, Raman activity and force constants are reported in Table 4. For visual comparison, the observed and calculated FTIR and FT-Raman spectra of 2,2,4-tribromoacetophenone at B3LYP level using 6-311++G(d,p) basis set are shown in Figs 2 and 3, respectively.

The main focus of the present investigation is the proper assignment of the experimental frequencies to

Table 2 — Definition of internal coordinates of 2,2,4-tribromoacetophenone

No. (i)	Symbol	Type	Definition
		Stretching	
1 – 4	r_i	C-H	C_2-H_{13}, C_3-H_{14}, C_5-H_{16}, C_6-H_{17}
5 – 7	R_i	CH(Methyl)	C_9-H_{10}, C_9-Br_{11}, C_9-Br_{12}
8	P_i	C-O	C_7-O_8
9	Q_i	C-Br	C_4-Br_{15}
10-17	q_i	C-C	C_1-C_2, C_2-C_3, C_3-C_4, C_4-C_5, C_5-C_6, C_6-C_1, C_1-C_7, C_7-C_9
		In-plane bending	
18-23	α_i	Ring	C_1-C_2-C_3, C_2-C_3-C_4, C_3-C_4-C_5, C_4-C_5-C_6, C_5-C_6-C_1, C_6-C_1-C_2
24-31	β_i	C-C-H	C_1-C_2-H_{13}, C_3-C_2-H_{13}, C_2-C_3-H_{14}, C_4-C_3-H_{14}, C_4-C_5-H_{16}, C_6-C_5-H_{16}, C_5-C_6-H_{17}, C_1-C_6-H_{17}
32	β_i	C-C-H	C_7-C_9-H_{10}
33, 34	β_i	C-C-Br	C_7-C_9-Br_{11}, C_7-C_9-Br_{12}
35-37	γ_i	Br-C-H	Br_{11}-C_9-H_{10}, H_{10}-C_9-Br_{12}, Br_{11}-C_9-Br_{12}
38-39	θ_i	C-C-C	C_6-C_1-C_7, C_2-C_1-C_7
40	θ_i	C-C-C	C_1-C_7-C_9
41-42	ϕ_i	C-C-Br	C_5-C_4-Br_{15}, C_3-C_4-Br_{15}
43-44	π_i	C-C-O	C_1-C_7-O_8, C_9-C_7-O_8
		Out-of-plane bending	
45-48	ω_i	C-H	H_{13}-C_2-C_1-C_3, H_{14}-C_3-C_4-C_2, H_{16}-C_5-C_6-C_4, H_{17}-C_6-C_5-C_4
49-50	ψ_i	C-C	C_7-C_1-C_6-C_2, C_9-C_7-C_1-(C_6, C_2)
51	λ_i	C-Br	Br_{15}-C_4-C_5-C_3
52	η_i	C-O	O_8-C_7-C_1-(C_6-C_2)
Torsion			
53-58	τ_i	t ring	C_1-C_2-C_3-C_4, C_2-C_3-C_4-C_5, C_3-C_4-C_5-C_6, C_4-C_5-C_6-C_1, C_5-C_6-C_1-C_2, C_6-C_1-C_2-C_3
59	τ_i	tC-CH_3	(Br_{11}, H_{10}, Br_{12})-C_9-C_7-C_1, (C_6, C_2)

Table 3 — Definition of local symmetry coordinates of 2,2,4-tribromoacetophenone

No. (i)	Type	Definition
1-4	CH	r_1, r_2, r_3, r_4
5	CH_3ss	$(R_5 + R_6 + R_7)/\sqrt{3}$
6	CH_3ips	$(2R_5 + R_6 + R_7)/\sqrt{6}$
7	CH_3ops	$(R_6 - R_7)/\sqrt{2}$
8	CO	P_8
9	CBr	Q_9
10-17	CC	q_{10}, q_{11}, q_{12}, q_{13}, q_{14}, q_{15}, q_{16}, q_{17}
18	Rtrigd	$(\alpha_{18} - \alpha_{19} + \alpha_{20} - \alpha_{21} + \alpha_{22} - \alpha_{23})/\sqrt{6}$
19	Rsymd	$(-\alpha_{18} - \alpha_{19} + 2\alpha_{20} - \alpha_{21} - \alpha_{22} + 2\alpha_{23})/\sqrt{12}$
20	Rasymd	$(\alpha_{18} - \alpha_{19} + \alpha_{21} - \alpha_{22})/2$
21-24	bCH	$(\beta_{24} - \beta_{25})/\sqrt{2}$, $(\beta_{26} - \beta_{27})/\sqrt{2}$, $(\beta_{28} - \beta_{29})/\sqrt{2}$, $(\beta_{30} - \beta_{31})/\sqrt{2}$
25	CH_3sb	$(-\beta_{32} - \beta_{33} - \beta_{34} + \gamma_{35} + \gamma_{36} + \gamma_{37})/\sqrt{6}$
26	CH_3ipb	$(-\gamma_{35} - \gamma_{36} - 2\gamma_{37})/\sqrt{6}$
27	CH_3opb	$(\gamma_{35} - \gamma_{36})/\sqrt{2}$
28	CH_3ipr	$(2\beta_{32} - \beta_{33} - \beta_{34})/\sqrt{6}$
29	CH_3opr	$(\beta_{33} - \beta_{34})/\sqrt{2}$
30	bCC	$(\theta_{38} - \theta_{39})/\sqrt{2}$
31	bCC	θ_{40}
32	bCBr	$(\theta_{41} - \theta_{42})/\sqrt{2}$
33	πCO	$(\pi_{43} - \pi_{44})/\sqrt{2}$
34-37	ωCH	ω_{45}, ω_{46}, ω_{47}, ω_{48}
38, 39	ψCC	ψ_{49}, ψ_{50}
40	λCBr	λ_{51}
41	ηCO	η_{52}
42	tRtrigd	$(\tau_{53} - \tau_{54} + \tau_{55} - \tau_{56} + \tau_{57} - \tau_{58})/\sqrt{6}$
43	tRsymd	$(\tau_{54} - \tau_{56} + \tau_{57} - \tau_{59})/\sqrt{2}$
44	tRasymd	$(-\tau_{54} + 2\tau_{55} - \tau_{56} - \tau_{57} + 2\tau_{58} - \tau_{59})/\sqrt{12}$
45	tCCH_3 twist	τ_{59}

the various vibrational modes of TBAP in collaboration with the calculated harmonic vibrational frequencies at the B3LYP level using the standard 6-311++G(d,p) basis set. The comparison of the frequencies calculated by B3LYP method with the experimental values reveals the overestimation of the calculated vibrational modes due to neglect of anharmonicity in real system. The vibrational analysis obtained for TBAP with the unscaled B3LYP force field is, generally, somewhat greater than the experimental values. These discrepancies can be corrected either by computing anharmonic corrections explicitly or by introducing a scaled field or directly scaling the calculated wavenumbers with proper factor. A tentative assignment is often made on the basis of the unscaled frequencies by assuming the observed frequencies so that they are in the same order as the calculated ones. Then, for an easier comparison to the observed values, the calculated frequencies are scaled by the scale to less than 1, to minimize the overall deviation. For that purpose, the scaling factor of 0.998 for all the fundamental modes has been utilized to obtain the scaled frequencies of the compound. The resultant scaled frequencies are also listed in Table 4.

C-H vibrations — Aromatic compounds commonly exhibit multiple weak bands in the region 3100-3000 cm^{-1} due to aromatic C-H stretching vibrations[17].

Table 4 —The observed FTIR, FT-Raman and calculated (Unscaled and Scaled) frequencies (cm^{-1}), force constant (mdyn A^{-1}), IR intensity (km/mol), Raman activity (Å amu^{-1}) and probable assignments (characterized by PED) of 2,2,4-tribromo acetophenone using DFT-B3LYP method with 6-311++G(d,p) basis set

Sl. No.	Observed frequencies (cm^{-1})		Calculated frequencies (cm^{-1}) by B3LYP/6-311++G(d,p) method					Assignment with PED(%) among types of internal coordinates
	FTIR	Raman	Unscaled	Scaled	Force constants	IR Intensity	Raman activity	
1	3207(vw)	-	3209	3203	6.6481	0.7703	222.4107	νCH(99)
2	-	3198(s)	3208	3201	6.6347	2.0480	9.8937	νCH(99)
3	-	3192(vw)	3196	3190	6.5510	1.1060	49.2840	νCH(98)
4	3095(vw)	-	3193	3187	6.5362	1.3292	29.7750	νCH(95)
5	3055(s)	-	3177	3170	6.4697	4.9857	32.6096	νCH(92)
6	1755(w)	1750(s)	1761	1757	22.5494	162.7227	171.0951	νCC(90)
7	1615(vs)	1620(vs)	1621	1618	8.4109	146.8523	317.9941	νCC(89)
8	1590(vs)	-	1598	1595	10.1108	27.9516	22.1295	νCC(86), bCH(14)
9	-	1515(vw)	1514	1511	2.9660	17.2139	2.7520	νCC(85), bCH(12)
10	1426(m)	1424(vw)	1425	1422	3.3458	27.6537	4.2786	νCC(84), Rtrigd(12)
11	1328(s)	-	1333	1330	1.5896	6.6145	1.0861	νCC(82), bCBr(15)
12	-	1315(w)	1323	1320	4.9834	5.1826	0.3638	νCC(80), Rtrigd(15)
13	1278(s)	-	1284	1281	1.9322	88.3650	11.6920	νCC(79), bCBr(16)
14	-	1202(m)	1210	1207	1.0599	73.1930	40.3424	νCO(76), bCO(16)
15	1200(s)	-	1207	1204	1.2919	56.5505	24.1344	bCH(75), bCBr(15)
16	-	1156(m)	1163	1160	0.9780	28.9130	40.7411	bCH(72), Rasymd(15)
17	1130(w)	1132(w)	1136	1133	1.0487	8.2356	7.5053	bCH(75), bCBr(17)
18	-	1078(m)	1084	1081	2.0402	71.2725	70.9836	bCH(73), Rsymd(19)
19	1022(s)	-	1026	1023	2.4062	29.1991	6.9761	bCH(72), bCBr(15)
20	-	1001(vw)	1002	1000	0.8212	4.8563	0.8372	Rtrigd(70), bCO (14)
21	-	982(w)	985	983	2.1479	99.6316	16.6098	Rsymd(68), bCH(15)
22	960(s)	-	968	966	0.7556	2.6808	0.4410	Rasymd(69), bCBr(15)
23	858(m)	-	861	859	0.7257	36.2384	0.3953	bCC(68), bCBr(14)
24	800(w)	802(w)	835	833	0.5566	6.7354	0.2406	bCC(65), Rasymd(19)
25	-	788(vw)	793	791	2.4660	23.8617	14.1455	bCO(66), bCBr(15)
26	755(vw)	750(vw)	763	761	1.0981	10.7756	3.5879	ωCH(64), bCC(18)
27	716(m)	712(vw)	722	720	2.0684	49.5739	7.3637	ωCH(63), bCC(15)
28	-	690(w)	702	700	1.3538	3.1574	3.2148	ωCH(62), bCO(19)
29	649(m)	-	653	651	1.8083	53.7754	29.0280	ωCH(62), bCC(18)
30	635(vw)	-	640	638	1.7156	1.1085	5.6529	ωCH(61), Rasymd(19)
31	551(m)	550(w)	551	550	1.2833	61.3227	17.9543	ωCC(60), bCC(18)
32	497(w)	497(vw)	501	500	0.8858	15.3006	0.6343	ωCC(61), tRasymd(12)
33	465(vw)	-	469	468	0.5347	5.1020	0.8565	ωCO(61), tRsymd(15)
34	-	406(vw)	412	411	0.2895	0.0850	0.0506	tRtrigd(64), ωCH(14)
35	-	355(vw)	362	361	0.4928	12.7486	0.3079	tRsymd(62), ωCH(16)
36	-	285(vw)	286	285	0.4875	0.1943	0.4216	tRasymd(61), ωCBr(19)
37	-	246(w)	253	252	0.2801	0.8007	1.9778	νCBr(69), bCH(14)
38	-	222(vw)	223	222	0.2492	0.8976	0.6366	νCBr(68), tRasymd(15)
39	-	195(vw)	196	195	0.9065	0.4434	6.6479	νCBr(67), tRsymd(12)
40	-	136(vw)	139	138	0.2786	1.5946	1.1179	bCBr(65), bCC(15)
41	-	130(w)	132	131	0.1627	1.0333	0.8886	bCBr(64), bCH(15)
42	-	86(vw)	86	86	0.0651	1.1448	0.3363	bCBr(64), bCC(15)
43	-	-	74	74	0.0347	0.8044	0.1504	ωCBr(59), tRasymd(15)
44	-	-	31	31	0.0030	0.0960	4.7666	ωCBr(60), tRsymd(12)
45	-	-	20	20	0.0031	0.0507	2.4116	ωCBr(61), tRtrigd(14)

Abbreviations: ν-stretching; ss – symmetric stretching; b-bending; ω-out-of-plane bending; R-ring; trigd-trigonal deformation; symd-symmetric deformation; asymd-antisymmetric deformation; t-torsion; s-strong; vs-very strong; ms-medium strong; w-weak; vw-very weak.

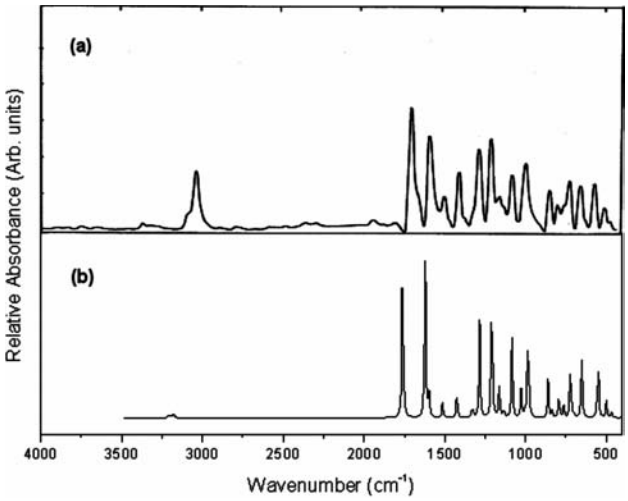

Fig. 2 — Comparison of observed and calculated IR spectra of 2,2,4-tribromoacetophenone (a) observed; (b) calculated with B3LYP/6-311++G(d,p)

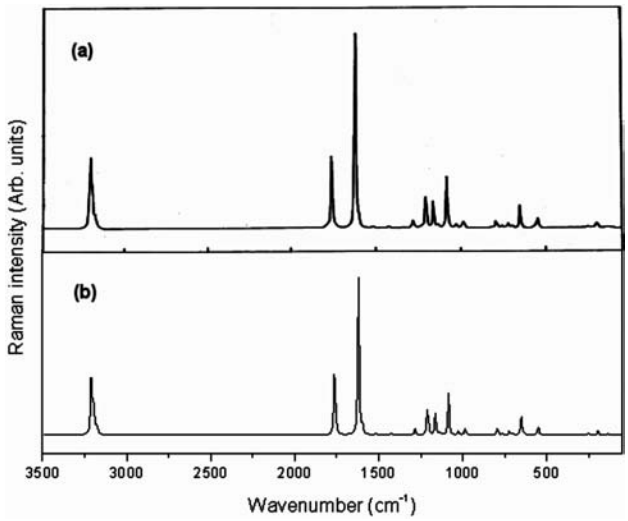

Fig. 3 — Comparison of observed and calculated Raman spectra of 2,2,4-tribromoacetophenone (a) observed; (b) calculated with B3LYP/6-311++G(d,p)

Hence, the infrared bands appeared at 3207, 3095 and 3055 cm^{-1} and the Raman bands found at 3198, 3192 cm^{-1} in TBAP have been assigned to C-H stretching vibrations and these modes are confirmed by their PED values. The bands due to C-H in-plane ring bending vibrations, interact somewhat with C-C stretching vibrations, are observed as a number of sharp bands in the region 1300-1000 cm^{-1}. The C-H out-of-plane bending vibrations are strongly coupled vibrations and occur in the region 900-667 cm^{-1}. The FT-Raman bands at 1156, 1132, 1078 cm^{-1} and infrared bands at 1200, 1130, 1022 cm^{-1} are assigned to C–H in-plane bending vibrations of TBAP. The out-of-plane bending vibrations of C-H group have also been identified for TBAP and are presented in Table 4. The theoretically computed values for C-H vibrational modes by B3LYP/6-311++G(d,p) method give excellent agreement with experimental data.

C=O vibrations — The carbonyl group vibrational frequencies are the significant characteristic bands in the vibrational spectra of ketones, and for this reason, such bands have been the subject of extensive studies[18]. The intensity of these bands can increase because of conjugation, therefore, leads to the intensification of the Raman lines as well as the increased infrared band intensities. The carbonyl stretching vibrations in ketones are expected in the region 1680-715 cm^{-1}. In this case, the band observed at 1202 cm^{-1} in FT-Raman spectrum is assigned as C=O stretching vibration and the corresponding force constant contributes 76% to the PED. The vibrational bands at 788 cm^{-1} and 465 cm^{-1} are assigned to C=O in-plane and out-of-plane bending vibrations for TBAP, respectively. These vibrational assignments are in line with the literature.

C–C vibrations — The C-C aromatic stretching vibrations give rise to characteristic bands in both the observed IR and Raman spectra[19], covering the spectral range from 1600 to 1400 cm^{-1}. Therefore, the C–C stretching vibrations of TBAP are found at 1755, 1615, 1590, 1426, 1328, 1278 cm^{-1} in FTIR and 1750, 1620, 1515, 1424, 1315 cm^{-1} in the FT-Raman spectrum, which are further supported by the high value of PED. Most of the ring vibrational modes are affected by the substitutions in the aromatic ring of TBAP. In the present study, the bands observed at 960 cm^{-1} and 1001, 982 cm^{-1} in the FTIR and Raman spectrum, respectively, have been designated to ring in-plane bending modes by careful consideration of their quantitative descriptions. The ring out-of-plane bending modes of TBAP are also listed in the Table 4. The reductions in the frequencies of these modes are due to the change in force constant and the vibrations of the functional groups present in the molecule.

C–Br vibrations — Strong characteristic absorption due to the C–Br stretching vibration is observed[20] with the position of the band being influenced by neighbouring atoms or groups, the smaller the halide atom, the greater the influence of the neighbouring atoms. Bands of weak to medium intensity are also observed for the C–Br stretching vibrations.

According to these early reports[21], the C–Br stretching vibration gives,generally, strong band in the region 650–485 cm^{-1}. In the present work, the Raman band is observed at 246, 222 and 195 cm^{-1} for C–Br stretching vibrations and this assignment is in line with the literature. In TBAP, the bands are assigned at 136, 130, 86 cm^{-1} for C–Br in-plane vibrations and out-of-plane bending vibrations are also listed in the Table 4. The theoretically computed values by B3LYP/6-311++G(d,p) method for C–Br in-plane bending nearly coincide with the experimental values. This shows that the other vibrations can hold back the C–Br vibrations due to its weak force constant. The influence of other substitution on C–Br stretching and deformation bands is significant in this compound.

4.3 Other molecular properties

Using the DFT/B3LYP with 6-311++G(d,p) basis set calculations, several thermodynamic properties like heat capacity, zero point energy, entropy of TBAP have been calculated and are presented in Table 5. Scale factors have been recommended for an accurate prediction in determining the zero-point vibration energy (ZPVE) and the entropy (S_{vib}). The variation in the ZPVE seems to be insignificant. The total energy and the change in the total entropy of the title compound at room temperature are also presented. All the thermodynamic data supply helpful information for further study on the TBAP. They can be used to compute the other thermodynamic energies according to relationships of thermodynamic functions and estimate directions of chemical reactions according to the second law of thermodynamics in thermochemical field.

Table 5 — Thermodynamic parameters of 2,2,4-tribromoacetophenone calculated at DFT-B3LYP method with 6-311++G(d,p) basis set

Parameters	Values by B3LYP method
Optimized global minimum Energy,(Hartrees)	-8105.61263698
Total energy(thermal), E_{total} (kcal mol^{-1})	75.130
Heat capacity, C_v(cal mol^{-1} k^{-1})	40.940
Entropy, S (cal mol^{-1} k^{-1})	
Total	118.065
Translational	43.484
Rotational	34.476
Vibrational	40.104
Zero point vibrational energy, (kcal mol^{-1})	67.6603
Rotational constants (GHz)	
A	0.9024
B	0.1238
C	0.1154

4.4 First hyperpolarizability

The quantum chemistry based on the prediction of non-linear optical (NLO) properties of a molecule has an important role for the design of materials in modern communication technology, signal processing and optical interconnections[22]. Especially, organic molecules are studied because of their larger NLO susceptibilities arising π-electron cloud movement from donor to acceptor, fast NLO response times, high laser damage thresholds and low dielectric constants. The components of dipole moment, polarizability and the first hyperpolarizability of the title compound can be seen in Table 6. The total static dipole moment μ, the average linear polarizability $\bar{\alpha}$, the anisotropy of the polarizability Δα, and the first hyperpolarizability β can be calculated by using the following equations[22]:

$$\mu = (\mu_x^2 + \mu_y^2 + \mu_z^2)^{1/2}$$

$$\bar{\alpha} = \frac{1}{3}(\alpha_{xx} + \alpha_{yy} + \alpha_{zz})$$

$$\Delta\alpha \frac{1}{\sqrt{2}}\{[(\alpha_{xx} - \alpha_{yy})^2 + (\alpha_{yy} - \alpha_{zz})^2 + (\alpha_{zz} - \alpha_{xx})^2 + 6\alpha_{xx}^2]\}^{1/2}$$

$$\beta=[(\beta_{xxx} + \beta_{xyy} + \beta_{xzz})^2 + (\beta_{yyy} + \beta_{xxy} + \beta_{yzz})^2 + (\beta_{zzz} + \beta_{xxz} + \beta_{yyz})^2]^{1/2}$$

The calculated values of total static dipole moment μ, the average linear polarizability $\bar{\alpha}$, the anisotropy of the polarizability Δα, and the first

Table 6 — Calculated dipole moment μ (Debye), polarizabi lity (α) and the first hyperpolarizability (β) components (a.u.) for 2,2,4-tribromo acetophenone

Components	Values	Components	Values
μ_x	2.1150	β_{xxx}	-1649.575
μ_y	0.8469	β_{xxy}	-143.572
μ_z	-1.6968	β_{xyy}	62.462
		β_{yyy}	65.241
α_{xx}	237.266	β_{xxz}	165.899
α_{xy}	10.320	β_{xyz}	-2.078
α_{yy}	136.437	β_{yyz}	-21.567
α_{xz}	-2.829	β_{xzz}	3.664
α_{yz}	-13.141	β_{yzz}	23.001
α_{zz}	115.014	β_{zzz}	-77.109

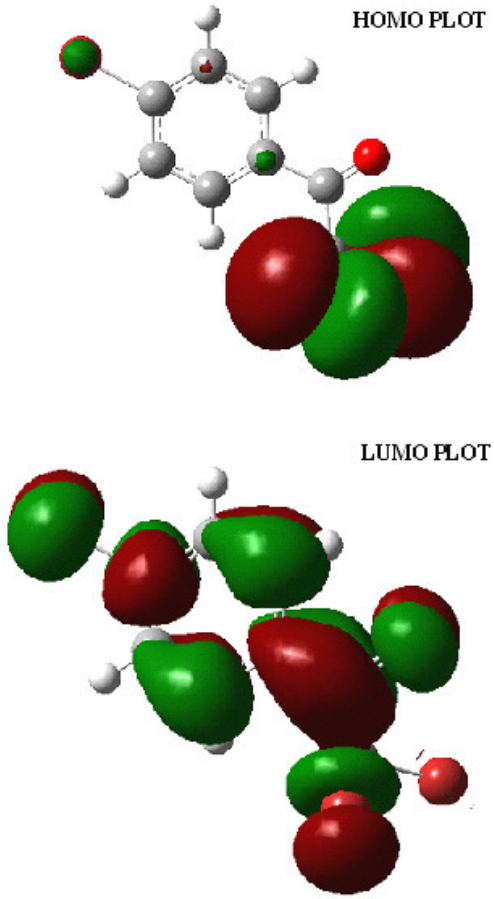

Fig. 4 — Atomic orbital HOMO and LUMO compositions of the frontier molecular orbital for 2,2,4-tribromoacetophenone

hyperpolarizability β using the DFT-B3LYP method are 2.8407 Debye, 24.1165 Å^3, 63.1084 Å^3 and 13.703×10^{-30} cm^5 e.s.u.$^{-1}$, respectively. The values of μ, $\bar{\alpha}$ and β obtained by Sun *et al*[23]. with the B3LYP/6-311++G(d,p) method for urea are 1.373 D, 3.831 Å^3 and 3.729×10^{-31} cm^5 e.s.u.$^{-1}$, respectively. The first hyperpolarizability of the title compound is 36 times greater than that of urea. According to the magnitude of the first hyperpolarizability, the title compound may be a potential applicant in the development of NLO materials.

4.5 HOMO-LUMO analysis

The highest occupied molecular orbitals (HOMOs) and the lowest-lying unoccupied molecular orbitals (LUMOs) are named as frontier molecular orbitals (FMOs). The FMOs play an important role in the electric and optical properties, as well as in UV–vis spectra and chemical reactions[24]. The atomic orbital HOMO and LUMO compositions of the frontier molecular orbital for TBAP computed at the B3LYP/6-311++G(d,p) are shown in Fig. 4. The LUMO: of π nature, (i.e. benzene ring) is delocalized over the whole C-C bond. By contrast, the HOMO is located over $CHBr_2$ group; consequently the HOMO→LUMO transition implies an electron density transfer to C–C bond of the benzene ring from $CHBr_2$ group. Moreover, these orbitals significantly overlap in their position of the benzene ring for TBAP. The HOMO–LUMO energy gap of TBAP reflects the chemical activity of the molecule. The LUMO as an electron acceptor represents the ability to obtain an electron and HOMO represents the ability to donate an electron. Moreover, a lower HOMO–LUMO energy gap explains the fact that eventual charge transfer interaction is taking place within the molecule and is calculated as:

HOMO energy =–0.27493 au
LUMO energy =–0.10569 au
HOMO-LUMO energy gap = 0.16924 au

5 Conclusions

The optimized geometries, harmonic vibrational wavenumbers and intensities of vibrational bands of TBAP have been carried out using the B3LYP method with the standard 6-311++G(d,p) basis set calculations. The theoretical results are compared with the experimental vibrations. The DFT based quantum mechanical approach provides the most reliable theoretical information on the vibrational properties of TBAP. The assignments of most of the fundamentals provided in the present work are believed to be unambiguous. The PED calculation regarding the normal modes of vibration provides a strong support for the frequency assignment. Therefore, the assignments proposed at higher level of theory with higher basis set with only reasonable deviations from the experimental values seem to be correct. The calculated HOMO and LUMO energies show that charge transfer occur within the molecule. Furthermore, the thermodynamic and total dipole moment properties of the compound have been calculated in order to get insight into the compound.

References

1 Griffin R N, *Photochem. Photobiol*, 7 (1968) 159.
2 Lindqvist L, *J Phys Chem,* 76 (1972) 821.
3 Anbusrinivasan P& Kavitha S, *Asian J Chem,* 20 (2) (2008) 979.
4 Anbarasu P & Arivazhagan M, *Indian J Pure & Appl Phys,* 49 (2011) 227.

5 Seth S K, Hazra D K, Monika Mukherjee & Tanusree Kar, *J Mol Struct*, 936 (2009) 277.
6 Pei K, Ma Y, Zheng X & Li H, *Chem Phys Lett*, 437 (2007) 153.
7 Frisch M J, Trucks G W, Schlegal H B, *et al., Gaussian 09, Revision A.02, Gaussian, Inc.*, Wallingford CT, 2009.
8 Becke A D, *J Chem Phys*, 98 (1993) 5648.
9 Lee C, Yang W & Parr R G, *Phys Rev*, B37 (1998) 785.
10 Pulay P, Fogarasi G, Pongor G, Boggs J E & Vargha A, *J Am Chem Soc*, 105 (1983) 7037.
11 Rauhut G & Pulay P, *J Phys Chem*, 99 (1995) 3093.
12 Fogarasi G & Pulay P, in: During J R (Ed.), *Vibrational Spectra and Structure*, Vol.14, Elsevier, Amsterdam, 1985, p.125 (chapter 3).
13 Fogarasi G, Zhou X, Taylor P W & Pulay P, *J Am Chem Soc*, 114 (1992) 8191.
14 Sundius T, *Vib Spectrosc*, 29 (2002) 89.
15 MOLVIB (V.7.0): *Calculation of Harmonic Force Fields and Vibrational Modes of Molecules*, QCPE Program No. 807 (2002).
16 Frisch A, Nielson A B & Holder A J, *Gaussview user manual, Gaussian Inc.*, Pittsburgh, PA 2009.
17 George S, *Infrared and Raman characteristic group frequencies – Tables and Charts,* Third ed., Wiley, Chichester, 2001.
18 Smith B, *Infrared Spectral Interpretation, A Systematic Approach*, CRC Press, Washington, DC, 1999.
19 Ramalingam S & Periandy S, *Spectrochim Acta,* 78A (2011) 835.
20 Arivazhagan M & Prabhakaran S, *Indian J Pure & Appl Phys,* 50 (2012) 26.
21 Krishnakumar V & Balachandran V, *Spectrochim Acta*, 61 A (2005) 1001.
22 Sajan D, Hubert J, Jayakumar V S & Zaleski J, *J Mol Struct*, 785 (2006) 43.
23 Sun Y X, Hao Q L, Wei W X, Yu Z X, Lu L D, Wang X & Wang Y S, *J Mol Struct,* (Theochem.) 904 (2009) 74.
24 Fleming I, *Frontier Orbitals and Organic Chemical Reactions*, Wiley, London, 1976.